Rev. Roum. Sci. Techn.– Électrotechn. et Énerg.
Vol. **66**, *1*, pp. 33–39, Bucarest, 2021

AN EFFICIENT CONTROL APPROACH OF VOLTAGE AND FREQUENCY REGULATION IN AN AUTONOMOUS MICROGRID

PANKAJ KUMAR[1], MOHIT KUMAR[2] , NITAI PAL[1]

Key words: Microgrid, Islanded operations, Distributed generation, Fuzzy logic and proportional-integral (PI) controller.

The sustainable development of a nation is highly dependent on remote area electrification, which consists of a majorly decentralized type of loads. To fulfil such energy demands, the microgrid is the emerging alternative that utilizes distributed energy sources. Microgrid performance parameters like voltage-frequency regulation, dynamic and steady-state response become very important when it is operating in islanded mode or under the load change conditions. In this paper, an improved efficient power control strategy, based on fuzzy gain scheduling of the conventional proportional-integral controller (FGSPI), is proposed for voltage-frequency control in an inverter-based distributed generation unit. The simulation results of the proposed control strategy are compared with the conventional PI controller under aforesaid conditions. The simulation responses show the effectiveness of the proposed control strategy to restore the stability of the microgrid even in islanded condition. The intelligent and smooth operation of the proposed controller shows better robust performance than the traditional controller in MATLAB/Simulink environment.

1. INTRODUCTION

To accelerate global sustainable development, distributed generation (DG) is the significant alternative to meet the decentralized energy demands [1]. The DG technologies are getting more focus due to the increasing environmental concerns and depleting conventional sources. Due to the developing perspective of distributed generation, a microgrid (MG) concept is becoming popular. A MG is a mixture of different DG sources having an interface with an electrical distribution linkage [2]. MG is a better way to realize the huge potential of DG, which uses various green energy resources, small power generating units and associated loads. The significant challenges of frequency and voltage control during MGs operation in grid-connected and islanded mode are serious concerns over its quality operation. Most DG systems require power electronic converters for power change and interconnection with a grid system. However, power electronics interface units are also preferred to utilize ideal control strategies. The pulse-width-modulated (PWM) DG systems and voltage source inverters (VSI) [3] are commonly used interface units in such scenarios. The inverter units become very crucial in DG systems for ideal control functions and reaching the desires power qualities [4, 5]. Figure 1 shows a grid-connected MG system having two micro-sources connected to a common bus. It demands a robust control methodology to achieve an improved execution to satisfy the power value requirements in the systems. A current control technique of the PWM-VSI [6] system is unique among the significant features of the recent power electronic converters where DG units stay interconnected with the grid. Therefore, there are two key classes of present-day controllers: (i) nonlinear type, which is centered on closed-loop current type PWM; [7] and (ii) linear type, which is centered on open-loop voltage type PWM [8]. The MG frequency and voltage control can be accomplished with the droop control method [9–11]. This technique is implemented via the inner current response loop in the nonlinear regulator. Moreover, hysteresis current control (HCC) is used for a three-phase grid-interconnect VSI type systems. The HCC [12] remunerates the current inaccuracy as well as provides PWM signals using a suitable vibrant response. The current is organized individually along with a control delay in the current control strategy, which results in an enormous current swell employing high total harmonic distortion [9]. The linear current regulator, which is centered on space vector PWM (SVPWM) [13], is an acceptable controller which compensates the error of current either using the proportional-integral (PI) [14] controller or else by the analytical control system. The compensation and PWM signal generation could be done independently. This type of controller displays an efficient steady-state response with a high-quality sinusoidal waveform and low current ripple.

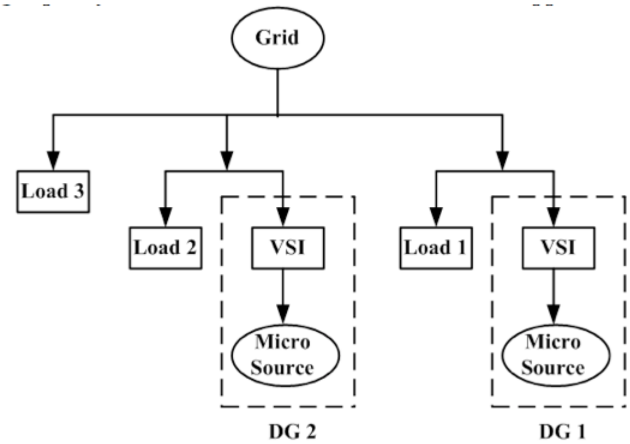

Fig. 1 – Layout of a grid-connected MG.

The DG system may use either of the twofold power control schemes: (a) active-reactive or (b) reactive-active power control scheme with grid-connected network mode [15]. However, the frequency-voltage control scheme can be used under the islanding mode of operation. During this case, the DG system is projected to deliver extreme power and uphold system constancy [16].

For better MG configuration [11, 12], scholars have examined power electronic controllers, which are based on an interior current control loop scheme. In [17], a controller has been presented, which seeks to confirm the system's stability and deliver complete information required for study and design. In [18], a novel distributed controller has been designed for secondary voltage and frequency control of an autonomous MG.

Fuzzy control is an important intelligent control technique that is increasingly being used for control problems [19]. In

[1] Department of Electrical Engineering, IIT (ISM), Dhanbad, India - 826004, pankaj.16dr000159@ee.ism.ac.in
[2] Department of Electrical Engineering, BTKIT, Dwarahat, India - 263653

this paper, an efficient power controller built on fuzzy tuning is presented for an inverter-based DG system in a MG. The controller, built on a synchronous reference frame, is interfaced using a current control loop. In this work, a conventional PI controller is used, and feed-forward compensation is given to an innermost control loop to get improved dynamic response. When the MG shifts either to load change or islanding mode condition, the proposed *V–f* control mode based fuzzy gain scheduled controller produces a robust response in terms of the system's voltage and frequency. The fuzzy gain scheduling method is used for real-time tuning of PI controller parameters, with integral time absolute error as a main objective function. The proposed effort aims to enhance the power quality by attaining the frequency and voltage within acceptable limits.

The work done in this paper comprises of five sections. In Section 2, the mathematical base of a three-phase grid-interconnect VSI model has been described. Section 3 deals with the power regulation scheme required in a MG. In Section 4, the proposed control scheme has been described. The simulation results have been analyzed in Section 5, and at last, the conclusion has been drawn in Section 6**.**

2. THREE-PHASE GRID-CONNECTED VSI SYSTEM

Figure 2 shows a three-phase systematic VSI model connected to a grid. The VSI is connected with an LC filter where L_s and R_s symbolize the equivalent lumped inductance and resistance of the filter, respectively. The capacitance of the filter and the voltage of the grid are indicated by C and V_s, respectively.

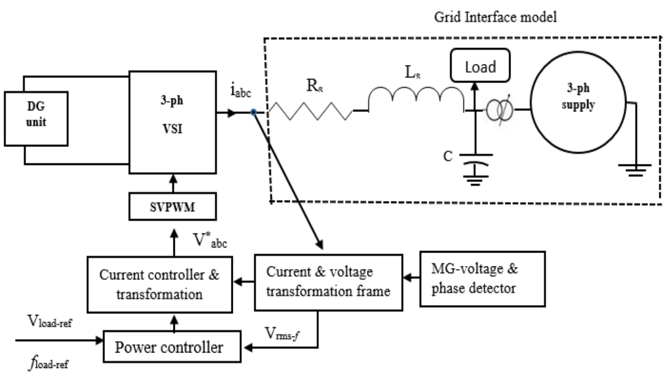

Fig. 2 – Three-phase grid-connected VSI model.

Considering the equivalent model, the state space equation of the system in the *abc* frame of reference [20] is given in equation (1) as follow.

$$\frac{\mathrm{d}}{\mathrm{d}t}\begin{bmatrix} i_a \\ i_b \\ i_c \end{bmatrix} = \frac{R_s}{L_s}\begin{bmatrix} i_a \\ i_b \\ i_c \end{bmatrix} + \frac{1}{L_s}\begin{bmatrix} V_{sa} \\ V_{sb} \\ V_{sc} \end{bmatrix} - \begin{bmatrix} V_a \\ V_b \\ V_c \end{bmatrix}, \quad (1)$$

where subscripts *s* and *a-b-c* denote the output value of the inverter and current, the voltage in *abc* frame of reference respectively. Now, converting equation (1) into *dq* reference frame by Park's transformation gives:

$$\frac{\mathrm{d}}{\mathrm{d}t}\begin{bmatrix} i_d \\ i_q \end{bmatrix} = \begin{bmatrix} \frac{-R_s}{L_s} & \omega \\ -\omega & \frac{-R_s}{L_s} \end{bmatrix}\begin{bmatrix} i_d \\ i_q \end{bmatrix} + \frac{1}{L_s}\left(\begin{bmatrix} V_{sd} \\ V_{sq} \end{bmatrix} - \begin{bmatrix} V_d \\ V_q \end{bmatrix}\right), \quad (2)$$

where ω in the above equation symbolizes coordinate angular frequency and subscript *d-q* represents the values in *dq* frame of reference. Similarly, Park's conversion can be given as:

$$i_{dq0} = T i_{abc} , \quad (3)$$

$$i_{dq0} = \begin{bmatrix} i_d \\ i_q \\ i_0 \end{bmatrix}, \quad i_{abc} = \begin{bmatrix} i_a \\ i_b \\ i_c \end{bmatrix} , \quad (4)$$

$$T = \sqrt{\frac{2}{3}}\begin{bmatrix} \cos\theta & \cos\left(\theta - \frac{2\pi}{3}\right) & \cos\left(\theta + \frac{2\pi}{3}\right) \\ -\sin\theta & -\sin\left(\theta - \frac{2\pi}{3}\right) & -\sin\left(\theta + \frac{2\pi}{3}\right) \\ \frac{1}{\sqrt{2}} & \frac{1}{\sqrt{2}} & \frac{1}{\sqrt{2}} \end{bmatrix}, \quad (5)$$

where $\theta = \omega_s t + \theta_0$ represents the synchronous rotating angle and θ_0 denotes the initial angle value.

3. V-F CONTROL STRATEGY

The main problems in the MG integrated with wind, and photovoltaic energy systems are their irregularities in the power generations, which are directly affected by the wind speed and solar irradiation, respectively. In his regards, DG units are categorized into three different energy resources- (i) variable speed resources like wind energy resource, (ii) high-speed resources like micro-turbine generators and (iii) direct energy such as fuel cells and photovoltaic system. Due to these reasons, a VSI is required to interface the DG resources to the grid and deliver a flexible operation [6]. The network of the VSI centered DG resource entity is connected along with the control configuration, as shown in Fig. 2. Hence, the controlled process of the DG unit depends on the inverter control mode. In grid-connected type system, the grid voltage is fixed. Therefore the frequency and voltage regulation is not essential, and DG units work as a PQ generating unit. Thus, the inverter must be able to track the reactive-active power (PQ) control mode. But, during the islanded condition, frequency, as well as voltage, is not fixed. Therefore, an effective power control mode may provide the high-performance operation of the DG units with a view that the DG resource units fulfill the load demand with good quality of power. For better and reliable MG functioning, it is required to confirm the different modes of operation and keep a balance between these operating modes in terms of varying voltage and frequency to satisfy the requirement of maintaining the system's voltage and frequency. For these cases, the V-f control scheme needs to be implemented to one or more DG resource units [6]. A schematic diagram based configuration of VSI based power controller is shown in Fig. 3.

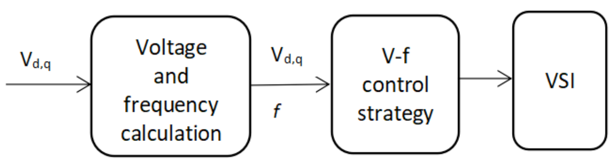

Fig. 3 – VSI based *V-f* power controller.

The rreference values for both the parameters (frequency and voltage) can be defined locally or by the MG control centre, where the phase-locked loop measures it.

4. **PROPOSED CONTROL STRATEGY**

For the three-phase grid-connected VSI system, the controller scheme has been shown in Fig. 4. The proposed controller includes three blocks - (i) power controller, (ii) current controller and (iii) fuzzy tuned PI controller. The functionality of each block is described in the following subsections.

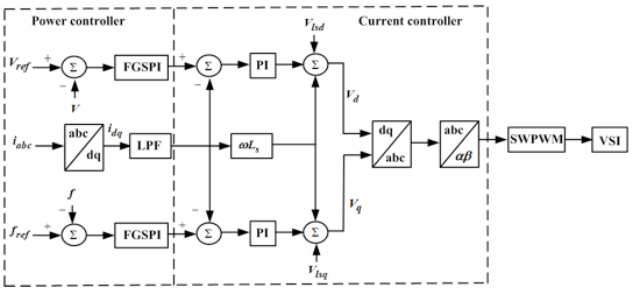

Fig. 4 – Proposed power controller scheme.

4.1 POWER CONTROL SCHEME

The power control scheme has been utilized to enhance the power quality of the system. To generate the reference current vectors (i_d^* and i_q^*), the outer control loop, which is based on two PI regulators, is shown in Fig. 4. A relatively small alteration in the reference current would make certain high quality of the inverter output power, which indicates that the control objective has been obtained. In this work, the *V–f* control scheme based on the fuzzy tuned PI strategy is projected for the VSI based DG unit. The main objective of the control scheme is to maintain frequency and the voltage, which must be attained for different working conditions (*i.e*, islanding mode or sudden load disturbances). The controller adjusts the frequency as well as the voltage according to their reference values (V_{ref} and f_{ref}). Moreover, the fuzzy tuning of parameters is an intelligent control processing that delivers optimal control parameters for providing desired reference current vectors. In this way, based on *dq* reference frame and two PI regulators, reference current vectors can be given as follow:

$$i_d^* = \left(V_{ref} - V\right)\left(K_{pv} + \frac{K_{iv}}{s}\right) , \tag{6}$$

$$i_q^* = \left(f_{ref} - f\right)\left(K_{pf} + \frac{K_{if}}{s}\right) . \tag{7}$$

4.2 CURRENT CONTROL SCHEME

Figure 4 shows the current control loop based on the synchronous reference frame. The main role of this loop is to ensure precise follow up and transient minimization of the inverter's output current. To execute Park's transformation in control scheme, the PLL block is used to sense the phase angle of the voltage. The grid voltage feed-forward loop and the current loop are employed to improve the steady-state and dynamic performance of the system by utilizing the PI controller, which results in the reduction of error. The controller's output signals are the reference voltage signals in the *dq* frame. By the inverse Clarke's and Park's transformation, it generates the reference voltage signals in αβ stationary frame, such that the controller produces pulses for the SVPWM to fire the insulated-gate bipolar transistor. According to equation (2), the reference voltage signals, in the synchronous *dq* frame, are expressed as:

$$\begin{bmatrix} V_d^* \\ V_q^* \end{bmatrix} = \begin{bmatrix} -K_p & -\omega L_s \\ \omega L_s & -K_p \end{bmatrix}\begin{bmatrix} i_d \\ i_q \end{bmatrix} + \begin{bmatrix} K_p & 0 \\ 0 & K_p \end{bmatrix}\begin{bmatrix} i_d^* \\ i_q^* \end{bmatrix} + \begin{bmatrix} K_i & 0 \\ 0 & K_i \end{bmatrix}\begin{bmatrix} X_d \\ X_q \end{bmatrix} + \begin{bmatrix} V_{sd} \\ V_{sq} \end{bmatrix} , \tag{8}$$

where the ‘‘*’’ denotes the reference values. The reference current vectors are: $\frac{\mathrm{d}X_d}{\mathrm{d}t} = i_d^* - i_d$ and $\frac{\mathrm{d}X_q}{\mathrm{d}t} = i_q^* - i_q$. By Clarke's transformation, equation (8) can be converted into αβ stationary frame as:

$$\begin{bmatrix} V_\alpha \\ V_\beta \\ V_0 \end{bmatrix} = \frac{2}{3}\begin{bmatrix} V_a \\ V_b \\ V_c \end{bmatrix}\begin{bmatrix} 1 & -\frac{1}{2} & -\frac{1}{2} \\ 0 & \frac{\sqrt{3}}{2} & -\frac{\sqrt{3}}{2} \\ \frac{1}{2} & \frac{1}{2} & \frac{1}{2} \end{bmatrix} . \tag{9}$$

Also, the inductor current can be achieved using a low pass filter (LPF) [17]. The LPF is expressed as the first-order transfer function as shown:

$$f\frac{1}{1 + sT_i} = f_l , \tag{10}$$

where *f*, f_l and T_i are denoted as the filter input value, filtered value and time constant, respectively.

4.3 FUZZY LOGIC CONTROLLER FOR PROPOSED POWER CONTROLLER

Fuzzy logic is a kind of tool which is used to reimburse the above mentioned teething trouble. It deals with inaccurate, unclear, or "fuzzy" evidence [7]. The decision-making process accomplishes to be a very pleasing performance despite the need for a mathematical model of the system. It works just by uniting the specialist facts into fuzzy [3]. Moreover, it compels the use of accurate declarations and precise values, hence making it more vigorous, denser, and modest.

The power controller is based on dual PI regulators for the design of fuzzy tuned PI-based power controller. Load end power deviation (Δ*V*) and its derivative are selected as inputs for the first FGPSI controller. Whereas load end frequency deviation (Δ*f*) and its derivative are selected as inputs vectors for the second FGPSI controller. Thus, fuzzy tuned PI controllers indicate an efficient control of the frequency and voltage to the system, as explained in later sections.

4.3.1 DESIGN OF HYBRID FUZZY-PI CONTROLLER

The conventional controller is more utilized in industrial applications in the last many decades due to its easy design and low cost. But, despite these benefits, the conventional controller results in poor performance when the control system is highly nonlinear and vaguely defined. Therefore, retaining the advantages of the PI controller, a fuzzy tuned PI controller is developed as shown in Fig. 5. The controller output is expressed as follow [21]:

$$u(t) = K_p \Delta u + K_i \int e(t)\,\mathrm{d}t , \tag{11}$$

where K_p and K_i are the proportional and integral gains of the conventional PI controller Δu and represents the output of the fuzzy logic controller. The inputs to the fuzzy logic system are error $e(t)$ and derivative of error $de(t)/d(t)$. The fuzzy tuning control structure of the controller has been shown in Fig. 5. The fuzzy logic controller involves the essentials components of fuzzification, Inference, fuzzy rule base, and defuzzification.

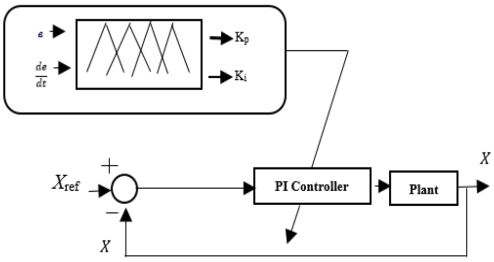

Fig. 5 – Configuration of fuzzy gain scheduled PI.

In this process, the input variables are mapped onto fuzzy variables. Every fuzzified variable occupies a definite membership function. Here, triangular membership functions have been designed for both input variables, as shown in Fig. 6. The input membership functions are represented by seven fuzzy sets namely, VS (very small), MS (medium small), S (small), Z (Zero), B (big), MB (medium big), and VB (very big).

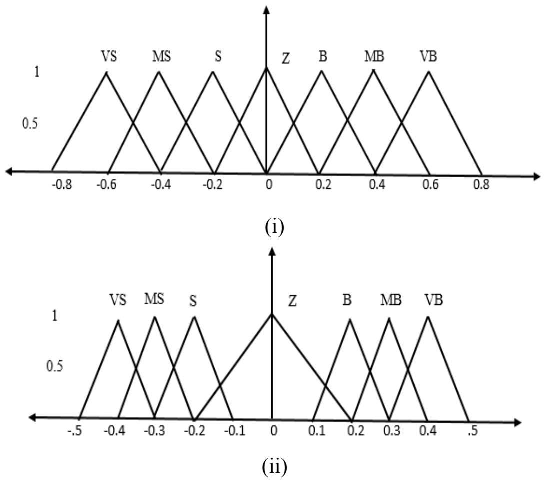

Fig. 6 – Membership functions of (i) $e(t)$ and (ii) $de(t)/d(t)$.

Concerning the fuzzified inputs, the inference mechanism used in the system delivers a set of control actions. In the present work, the Mamdani type interface mechanism has been used to regulate the degree of membership function of output variables.

Table 1

Fuzzy rule for FGSPI controller

$e \rightarrow$ / $\frac{de}{dt} \downarrow$	**VS**	**MS**	**S**	**Z**	**B**	**MB**	**VB**
VS	VS	VS	VS	Z	MS	S	SB
MS	VS	VS	VS	Z	Z	SB	MB
S	VS	VS	MS	Z	Z	MB	B
Z	VS	MS	S	Z	MB	B	VB
B	MS	S	Z	Z	B	VB	VB
MB	S	Z	S	Z	VB	VB	VB
VB	Z	S	MS	Z	VB	VB	VB

As per the desired transient and steady-state responses of the system, an appropriate fuzzy rule base has been developed, as shown in Table 1.

Finally, the process of defuzzification generates an output crisp set using the centroid of area method. The total area of the membership function distribution *i.e.*, {S, Z, B} utilized to perform the combined control action which is divided in different sub-areas. The area and centroid of each different sub-areas are further determined to obtained the defuzzified output crisp value. The corresponding mathematical expression is shown in equation (12).

$$X^* = \frac{\int x \mu_x(x)\,\mathrm{d}x}{\int \mu_x(x)\,\mathrm{d}x}, \qquad (12)$$

where $\mu_x(x)$ denotes the membership function, x is the sample element, and X^* represents defuzzified crisp output.

5. SIMULATION RESULTS

A three-phase grid-connected VSI system with the proposed FGSPI controller is simulated under MATLAB/ Simulink environment. The system parameters are taken as: L_s = 5 mH, R_s= 1.4 Ω, f = 50 Hz, filter capacitance C = 1500 μF and input capacitance of the dc side is fixed as 5000 μF. One DG unit of rating 180 kW is connected to the system. However, the load of the system has been taken as 150 kW. Typically, current control parameters K_p and K_i are taken as 7 and 10, respectively. In this case, the switching and sampling frequency of the SVPWM based current controller is fixed at 10 kHz and 500 kHz, respectively. To validate the robust efficient capability of the proposed controller, the following case studies are investigated for the MG system under investigation.

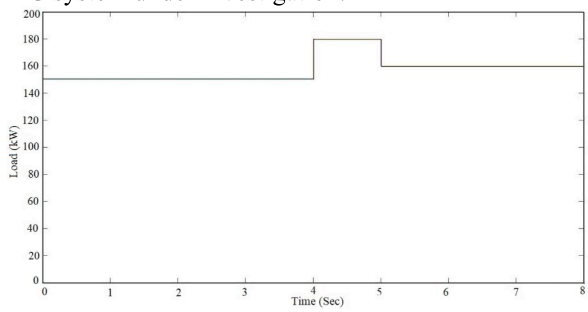

Fig. 7 – System's load variation.

5.1 VARIATION IN LOAD

For the evaluation of the proposed control scheme, the simulation has been performed in the grid-connected mode. At the 4th second, a load of 30 kW is injected and, at 5th second load of 20 kW is rejected at the distribution side, as shown in Fig. 7. Sudden load increment and rejection causes sag and swell in the voltage and frequency profile of the system, respectively. Figure 8 shows the results of different performance parameters for these conditions when a traditional PI controller is used. However, Fig. 9 shows an efficiently improved response when the proposed FGSPI controller is used in the power controller.

The system responses confirm that the proposed controller responds well to regulate the voltage and frequency of the system during load disturbances. It is being observed that a sudden dip of 4.5% in the rms voltage takes place during the inclusion of the load when the conventional PI controller is used. The voltage is further recovered by 2.5 % at the 5th second when 20 kW load is rejected. On the other hand, though a sudden voltage dip of

6.25 % has been observed in case of the proposed controller, but the system recovers back to its original voltage profile within a fraction of second. It also responds well in case of load rejection scenario. The time taken to stabilize the system voltage in case of load rejection is lesser than that of the load addition.

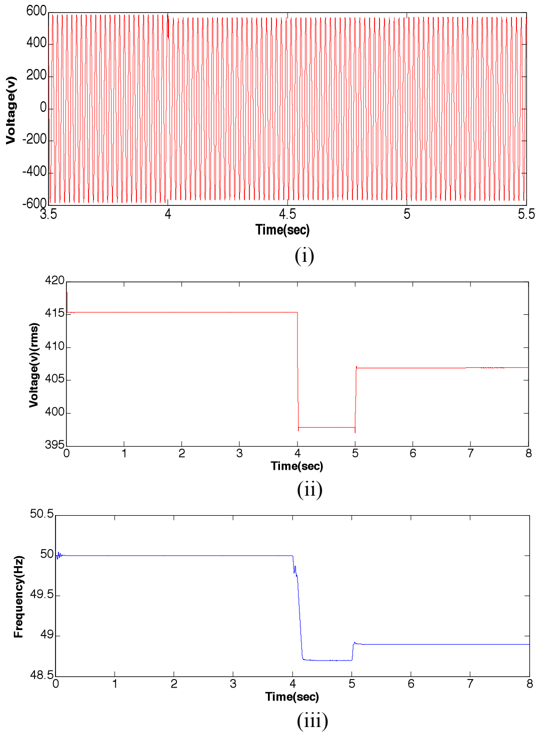

Fig. 8 – Load side parameters when PI controller is present, (i) line voltage, (ii) rms voltage, (iii) frequency.

The dynamic frequency response of the proposed controller is highly appreciated with the injection of load at 4th second.

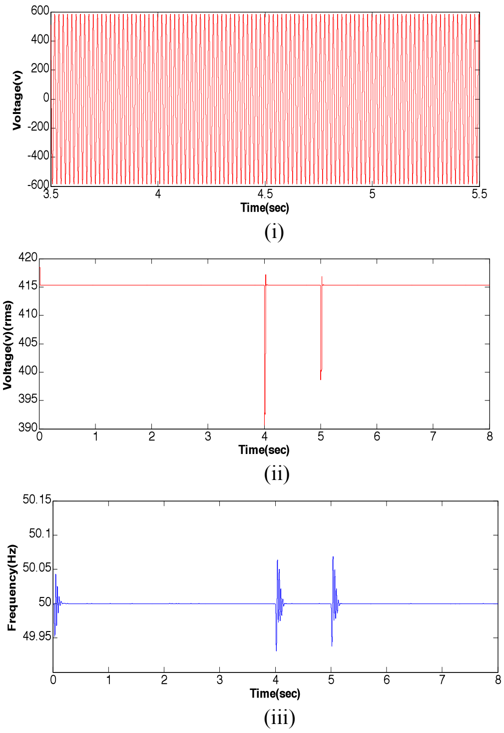

Fig. 9 – Load side parameters when FGSPI controller is present, (i) line voltage, (ii) rms voltage, (iii) frequency.

Figure 9(iii) shows that system's frequency stabilizes quickly after 0.21 s as soon as the perturbation is given to the load of the system at 4th second. Similarly, when the 20 kW load is discontinued from the system, the proposed controller pulls back to its original frequency mode after 0.22 s. In the case of the PI controller, system's frequency stabilizes at 48.71 Hz (with a deviation of –1.29 Hz) after 0.23 s from the applied load perturbation at the 4th second. During load discontinuation, the controller operates to minimize the deviation in system's frequency and stabilizes it at the level of 48.90 Hz (with a deviation of –1.1 Hz) after 0.07 s, as shown in Fig. 8(iii).

5.2 ISLANDED CONDITION

It has been considered that due to some abnormal condition, the grid gets disconnected with the DG units and the connected loads. This situation is called islanded condition. At the 4th second, the MG switches to the islanding operation mode and no other disturbances of load occur. Due to grid disconnection, which was primarily responsible for maintaining voltage and frequency profiles, a significant deviation of voltage and frequency occurs, as shown in Fig. 10. Now, the controller comes into action to eliminate this perturbation in frequency and voltage during islanding condition. It tries to restore the voltage and frequency within the acceptable limits. The islanding condition results are shown in Fig. 10 and Fig. 11 when PI and FGSPI controllers are used, respectively.

When the grid disconnection occurs, a 26.92 % dip in the voltage has been observed at the 4th second. But the voltage profile is regained to some extent due to the action of the PI controller. The restored rms voltage contains harmonics, and an enormous transient swing in the voltage has been observed from 4th to 5th second. On the other hand, a 25.48 % dip in the system's voltage is observed when the proposed controller works.

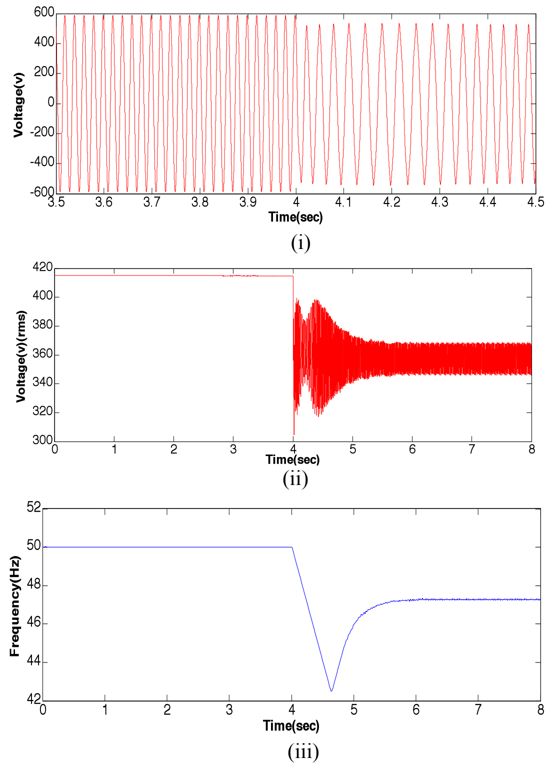

Fig. 10 – Load side parameters when PI controller is present (i) line voltage (ii) rms voltage (iii) frequency.

The controller recovers back to its original voltage level after the 48 ms of the grid disconnection, as shown in

Fig. 11(ii). Hence, the proposed controller's performance for the voltage restoration is exceptionally superior to that of the PI controller in case of grid disconnection.

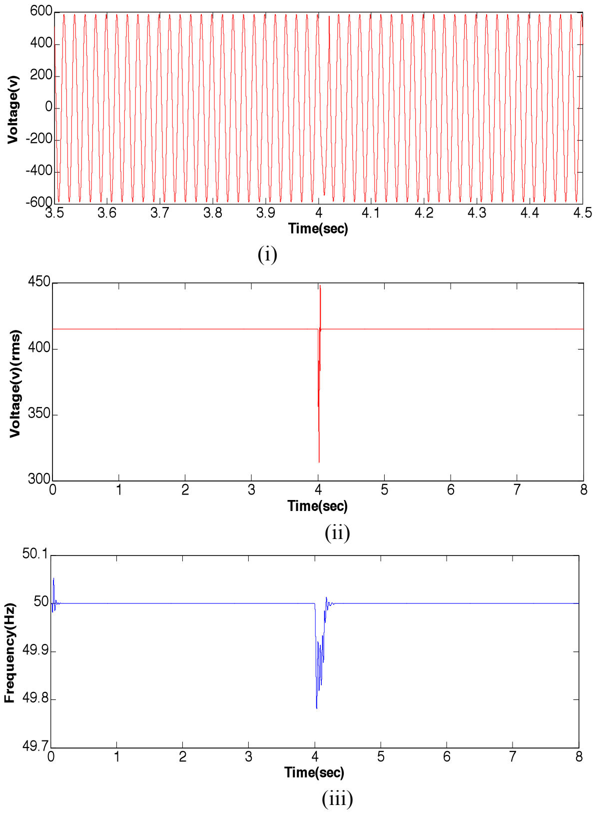

Fig. 11 – Load side parameters when FGSPI controller is present, (i) line voltage, (ii) rms voltage, (iii) frequency.

As shown in Fig 10(iii) and 11(iii), the frequency response of the proposed controller is much superior to that of the PI controller. When grid disconnection occurred at 4th second, a maximum frequency fluctuation of 15.2 % has been observed in the system's frequency during the operation of the traditional controller. Further, it has been partially recovered back by the controller with a frequency deviation of 5.34 % at steady state. Moreover, the effectiveness of the proposed controller can be assessed with the fact that it allows a maximum frequency deviation of 0.44 % during the grid disconnection, which is on acceptable limits. Also, it resumes backs the system's frequency at its standard value just after the 0.24 second of the islanding of the system.

It is evident from the obtained results that the FGSPI controller shows better dynamic and steady state performance and can attain its nominal voltage and frequency profile compared to the conventional PI controller during variation of load and islanded conditions. The corresponding performances of the controllers are also highlighted in Table 2. In the case of load addition, the settling time of the proposed controller to regain its original voltage profile is 0.05 second with the overshoot of 0.42 %. However, the settling time and overshoot during frequency regulation are 0.21 second and 0.12 %, respectively. When load disconnection occurs, the recovery times are obtained as 0.04 second and 0.22 second for the voltage and frequency regulation of the system, respectively. The corresponding overshoots are observed as 0.31 % and 0.14 %, respectively. At the same time, the voltage and frequency recovery time of the proposed controller in the case of islanding are obtained as 48 milliseconds and 0.24 second, respectively. While the corresponding voltage and frequency overshoot are found to be 8.17 % and 0.02 %, respectively. Additionally, comparing from the existing works of the distinguished researchers reveal that the recovery time and overshoot of the proposed controller are better from shown results by Kumar *et al.*, [22], Jumani *et al.*, [23], Esmaeili *et al.*, [24] and Rajamand [25]. Also, the obtained performance of the proposed controller is found to be comparable with the performance of the existing controllers in [26, 27].

It is worth mentioning here that the size of the frequency deviation and RoCoF also determine the satisfactory frequency response of the controller during load disturbances and islanding. Consequently, the system should be secured from frequency deviation and RoCoF limit. The steady-state response of the proposed controller denies any deviation in frequency ensuring the stability of the system after disturbances at 4th and 5th second.

Table 2

Comparative performance analysis of proposed control scheme with PI control scheme.

Characteristics parameters	**PI controller**	**FGSPI controller**
Variation of load:		
Voltage regulation after load addition	Shows deviation	Fully recovers
Frequency regulation after load addition	Shows deviation	Fully recovers
Voltage regulation after load rejection	Partially recovers	Fully recovers
Frequency regulation after load rejection	Partially recovers	Fully recovers
Grid disconnection:		
Voltage regulation	Large transient swing, partially recovers	Less transient swing, fully recovers
Frequency regulation	Large frequency deviation, partially recovers	Small frequency deviation, fully recovers

In the proposed work, to avoid switching harmonics in the inverter output, the filter has been used. The LPF with low enough cut-off frequency can provide sufficient attenuation for the harmonics of the *dq* current vectors.

6. CONCLUSION

In this paper, an improved, efficient fuzzy based power control scheme has been proposed for an inverter-based DG unit in a MG system. To improve the voltage and the frequency profile of the power supply, especially when the MG transits to the islanding operation mode or during load change, the FGSPI scheme has been incorporated into the *V-f* control mode. The simulation results indicate that the proposed FGSPI intelligent control scheme provides an excellent performance compare to the conventional controller PI for regulating the MG voltage and frequency and achieves a short transient time with a suitable level. Therefore, the proposed control strategy may be utilized by the grid interface DG unit in a MG scenario, considering the power-sharing issue.

Received on September 1, 2019

REFERENCES

1. G. Chen, F. L. Lewis, E. N. Feng, Y. Song, *Distributed optimal active power control of multiple generation systems*, IEEE Transaction on Industrial Electronics, **62**, *11*, pp. 7079–7090 (2015).
2. Y. Lim, H. Kim, *Strategic bidding using reinforcement learning for load shedding in MG*, Computer and Electrical Engineering, **40**, *5*, pp. 1439–1446 (2014).
3. R. C. Bansal, *Bibliography on fuzzy sett theory application to power systems*, IEEE Transaction on Power System, **18**, *4*, pp. 1291–1299 (2003).
4. J. Peter, M. S. KP, L. R, L. Ramchand, *Nearly constant switching space vector based hysteresis controller for VSI fed IM drive*, IEEE Transaction on Industry Application, **54**, *4*, pp. 3360–3371 (2018).
5. W. Li, X. Zhang, *Simulation of the smart grid communications: Challenges, techniques, and future trends*, Computers and Electrical Engineering, **40**, *1*, pp. 270–288 (2014).
6. Y. Mohamed, *New Control Algorithms for the Distributed Generation Interface in Grid-connected and Micro-grid Systems*, PhD thesis University of Waterloo, Ontario – Canada, 2008, p. 87–115.
7. C. C. Lee, *Fuzzy logic in control systems: fuzzy logic controller Part I*, IEEE Transaction on System, Man Cybernetics, **20**, *2*, pp. 404–418 (1990).
8. G. J. Castillo, F. J. M. Rodriguez, C. R. Casas, J. C. Hernandez, G. M. Tina, *Monitoring PWM signals in standalone photovoltaic systems*, Measurement, **134**, *4*, pp. 412–425 (2019).
9. J. A. P. Lopes, C. L. Moreira, A. G. Madureira, *Defining control strategies for MGs islanded operation*, IEEE Transaction on Power System, **21**, *2*, pp. 916–924 (2006).
10. B. Awad, J. Wu, N. Jenkins, *Control of distributed generation*, Elektrotechnik und Informationstechnik, **125**, *12*, pp. 409–414 (2008).
11. H. Bevrani, S. Shokoohi, *An intelligent droop control for simultaneous voltage and frequency regulation in islanded MGs*, IEEE Transaction on Smart Grid, **4**, *3*, pp. 1505–1513 (2013).
12. H. Bevrani, F. Habibi, P. Babahajyani, M. Watanabe, Y. Mitani, *Intelligent frequency control in an AC MG: Online PSO-based fuzzy tuning approach*, IEEE Transaction on Smart Grid, **3**, *4*, pp. 1935–1944 (2012).
13. R. H. Lasseter, J. H. Eto, B. Schenkman, J. Stevens, H. Vollkommer, D. Klapp, E. Linton, H. Hurtado, J. Roy, *CERTS MG laboratory test bed*, IEEE Transactions on Power Delivery, **26**, *1*, pp. 325–332 (2011).
14. M. Mokhtari, F. Aminifar, D. Nazarpour, S. Golshannavaz, *Wide-area power oscillation damping with afuzzy controller compensating the continuous communication delays*, IEEE Transactions on Power Systems, **28**, *2*, pp. 1997–2005 (2013).
15. N. Mohsenifari, A. Kargar, N. R. Abjadi, *Improved cascade sliding mode for power control in a MG*, Rev. Roum. Sci. Techn. – Électrotechn. Et Énerg., **61**, *4*, pp. 430–435 (2016).
16. H. Zhao, M. Hong, W. Lin, K. A. Laparo, *Voltage and frequency regulation of MG with battery energy storage systems*, IEEE Transaction on Smart Grid, **10**, *1*, pp. 414–424 (2019).
17. W. Deng, X. Tang, Q. Zhiping, *Research on dynamic stability of hybrid wind/PV system based on micro-grid*, International Conference on Electrical Machines and Systems (ICEMS), pp. 2627-2632, (2008).
18. J. W. S. Porco, Q. Shafiee, F. Dörfler, J. C. Vasquez, J. M. Guerrero, F. Bullo, *Secondary frequency and voltage control of islanded MGs via distributed averaging*, IEEE Transactions on Industrial Electronics, **62**, *11*, pp. 7025–7038 (2015).
19. C. Chowdary, S. P. Chowdhury, P. Crossley, *MGs and Active Distribution Networks*, London, The Institution of Engineering and Technology, U. K. – London, 2009, p. 75–211.
20. I. Y. Chung, W. Liu, D. A. Cartes, K. Schoder, *Control parameter optimization for a MG system using particle swarm optimization*, International Conference on System Engineering and Technology (ICSET), pp. 837–842 (2008).
21. M. A. Nezhad, H. Bevrani, *Frequency control in an islanded hybrid MG using frequency response analysis tools*, IET Renewable Power Generation, **12**, *2*, pp. 227-243, (2018).
22. T. B. Kumar, M. U, *Vani, Load frequency control in two area power system using ANFIS,* Computer Engineering and Intelligent Systems, **5,** pp. 27-35 (2014).
23. T. A. Jumani, M. W. Mustafa, M. M. Rasid, N. H. Mirjat, Z. H. Leghari, M. S. Saeed, *Optimal voltage and frequency control of an islanded microgrid using grasshopper optimization algorithm,* Energies, **11**, *11*, pp. 3191 (2018).
24. M. Esmaeili, H. Shayeghi, M. Nooshyar, H. Aryanpour, *Design of new controller for load frequency control of isolated microgrid considering system uncertainties,* **9**, 3, pp. 285-294 (2018).
25. S. Rajamand, *Effective Control of Voltage and Frequency in Microgrid Using Adjustment of PID Coefficients by Metaheuristic Algorithms,* pp. 1–14 (2021).
26. T. Rajesh, B. Gunapriya, M. Sabarimuthu, S. Karthikkumar, R. Raja, M. Karthik, *Frequency control of PV-connected micro grid system using fuzzy logic controller,* Materials Today: Proceedings, (2020).
27. M. H. Khooban, T. Niknam, M. Shasadeghi, T. Dragicevic, F. Blaabjerg, *Load frequency control in microgrids based on a stochastic noninteger controller,* IEEE Transactions on Sustainable Energy, **9,** *2*, pp. 853-861 (2017).